Peptide Stapling with Anion-π Catalysts

Pham, Anh Tuan; Matile, Stefan

How to cite

PHAM, Anh Tuan, MATILE, Stefan. Peptide Stapling with Anion-π Catalysts. In: Chemistry (Asian Journal), 2020, vol. 15, n° 10, p. 1562–1566. doi: 10.1002/asia.202000309

This publication URL: https://archive-ouverte.unige.ch/unige:135871
Publication DOI: 10.1002/asia.202000309

Peptide Stapling with Anion-π Catalysts

Anh-Tuan Pham and Stefan Matile*[a]

Abstract: We report design, synthesis and evaluation of a series of naphthalenediimides (NDIs) that are bridged with short peptides. Reminiscent of peptide stapling technologies, the macrocycles are conveniently accessible by a chromogenic nucleophilic aromatic substitution of two bromides in the NDI core with two thiols from cysteine sidechains. The dimension of core-bridged NDIs matches that of one turn of an α helix. NDI-stapled peptides exist as two, often separable atropisomers. Introduction of tertiary amine bases in amino-acid sidechains above the π-acidic NDI surface affords operational anion-π catalysts. According to an enolate chemistry benchmark reaction, anion-π catalysis next to peptides occurs with record chemoselectivity but weak enantioselectivity. Catalytic activity drops with increasing distance of the amine base to the NDI surface, looser homocysteine bridges, mismatched, shortened and elongated α-helix turns, and acyclic peptide controls. Elongation of isolated turns into short α helices significantly increases activity. This increase is consistent with remote control of anion-π catalysis from the α-helix macrodipole.

Anion-π enzymes have been introduced recently as artificial enzymes that operate with anion-π interactions.[1] This is unusual because all ribosomal aromatic amino-acid residues are π basic, that is suitable to stabilize cationic transition states[2] on their π surface.[3] As a result, cation-π enzymes are ubiquitous in biosynthesis, most impressively represented by the cyclization of terpenes into steroids,[4] and this conventional cation-π catalysis is also increasingly recognized as useful in organic synthesis.[5] In sharp contrast, anion-π catalysis,[3] that is transition-state stabilization[2] with anion-π interactions[6] on aromatic surfaces, is essentially missing in biology and has been introduced explicitly

in chemistry only recently.[7] Since then, anion-π catalysis has been confirmed for hexafluorobenzene,[8] NDIs,[3,9] perylenediimides (PDIs),[8] fullerenes,[3,8] carbon nanotubes,[10] π-stacked foldamers,[3] coated electrodes at high voltage[3] and anion-π enzymes[1] as catalysts,[3] and for reactions covering enolate, iminium and enamine chemistry, transamination, nonadjacent stereocenters, cascade reactions, Diels-Alder cycloadditions, and autocatalytic epoxide-opening ether cyclizations.[3,8,11]

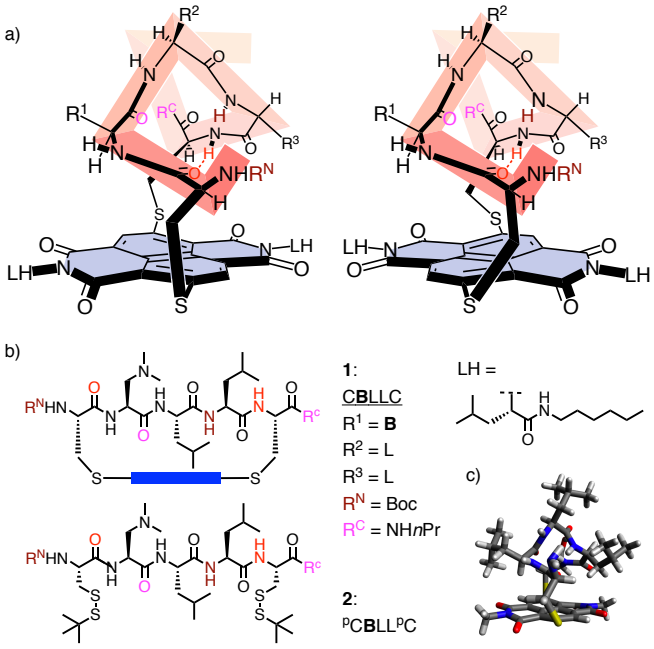

Figure 1. (a) General structure of a pair of atropisomers (diastereomers) of NDI-stapled peptides. Red: Peptide backbone in formal α-helical conformation, from (c). See Table 1 for specific structures. (b) Full structure of cyclic catalyst **1** and acyclic precursor **2**, (c) Molecular model of a general hypothetical structure (X = Y = Z = CH, Me instead of LH).

Anion-π enzymes were created by screening biotinylated anion-π co-factors against streptavidin mutant libraries.[1] The outstanding performance of the best mutant proteins called for the study of anion-π catalysts next to simple small peptides. To elaborate on this new topic for anion-π catalysis,

we designed, synthesized and characterized peptide-bridged[12,13] NDIs or NDI-stapled[14-16] peptides, plus the corresponding acyclic controls, i.e. catalysts **1**–**19** (Figure 1, Table 1).

Table 1. Characteristics of catalysts.[a]

Cat[b]	Sequence[c]	R^{C}[d]	qAD[e]	A/D[f]	*er*[g]
1	CB**B**LLC	NH*n*Pr	0.94	35	65:35
2	^{p}C**B**LL^{p}C	NH*n*Pr	–0.12	3	41:59
3	CB**B**LL^{h}C	NH*n*Pr	0.40	10	54:46
4	^{h}C**B**LL^{h}C	NH*n*Pr	0.18	6	55:45
			0.51	13	54:46
5	C**B**LC	NH*n*Pr	0.18	6	46:54
6	LC**B**LC	NH*n*Pr	0.35	9	45:55
7	C**B**LLLC	NH*n*Pr	0.30	8	52:48
8	C**B**LLC	NHAd	0.72	21	61:39
9	^{p}C**B**LL^{p}C	NHAd	0.10	5	43:57
10	C**B**LLCL	NHAd	0.97	37	58:42
11	^{p}C**B**LL^{p}CL	NHAd	–0.12	3	43:57
12	C**B**LLCLL	NHAd	1.20	63	56:44
13	^{p}C**B**LL^{p}CLL	NHAd	–0.12	3	43:57
14	CL**B**LC	NH*n*Pr	0.00	4	66:34
15	^{p}CL**B**L^{p}C	NH*n*Pr	0.18	6	49:51
16	CL**B**LC	NHAd	0.25	7	61:39
17	CLL**B**C	NH*n*Pr	0.68	19	48:52
			0.60	16	49:51
18	^{p}CLL**B**^{p}C	NH*n*Pr	0.30	8	49:51
19	CLL**B**C	NHAd	0.70	20	36:64
TEA			0.00	4	50:50

[a] Reactions were conducted as in Figure 2 and followed by ^{1}H NMR spectroscopy. [b] Catalysts; see Figures 1 and 3 for pertinent examples of full structures. Two data sets for one compound indicates that two atropisomers (diastereomers) have been isolated and characterized. [c] Peptide sequences, single letter abbreviations (L, L-leucine, C, L-cysteine; ^{h}C, L-homocysteine; ^{p}C, protected C (S*t*Bu); **B**, *S*-3-dimethylamino-2-aminopropionic acid); R^{N}, Boc. Sequences of cyclic peptides are underlined. [d] C-terminal substituents. [e] qAD = log (A/D) – log $(A/D)_0$. [f] Yield of addition product **26** divided by yield of decarboxylation product **27** at full substrate conversion. $(A/D)_0$: A/D with TEA as catalyst (A/D = 4.0, $\log(A/D)_0 = 0.60$). [g] Enantiomeric ratio.

For general catalyst design, we noticed that unlike imide-bridged NDIs,[12] the dimensions of core-bridged NDIs would match those of one turn of an α helix[14,15,17] (Figure 1c). To bridge or "staple"[14,15] a formal α-helix turn, dibromo NDIs **20** were easily accessible from dianhydride **21** and amines such as LH **22** (Schemes 1, S1-S10).[3,8] Nucleophilic substitution with two thiols from cysteine residues has been used before as convenient method to staple α helices[15] or to create bicyclic peptide libraries for screening.[16] The corresponding nucleophilic aromatic substitution of the bromines in **20** with the two thiols as in C**B**LLC pentapeptide **23** afforded the cyclic peptides such as <u>C**B**LLC</u> **1**.

Macrocyclization could be easily followed and the resulting macrocycles could be easily identified and purified because of the bright red color of NDIs with two sulfides in the core. Stapling yields up to 27% for **14** were determined. However, most reported macrocyclization yields are underestimates because sufficient purity of the final product for good quality data on catalytic performance was judged more important than high yields. Much material was thus sacrificed during purification, and the resulting yields were not further optimized because this was not the purpose of the study. Given the chromogenic nature of the macrocyclization, nucleophilic aromatic substitution in the NDI core could thus be of general interest for peptide stapling.

In <u>C**B**LLC</u> **1**, the CxxxC motif was chosen to staple one formal α-helix turn (Figure 1). In this sequence, amino acid residues are given with single-letter abbreviations, that is L for L-leucine, C for L-cysteine, ^{h}C for L-homocysteine, ^{p}C for protected L-cysteine (S*t*Bu), **B** for *S*-3-dimethylamino-2-aminopropionic acid. Sequences of cyclic peptides are underlined. Sequences are given from N to C terminus. N and C termini were converted into different charge-free amides. In <u>C**B**LLC</u> **1**, the artificial amino acid **B** was integrated to place a tertiary amine base near the catalytic π surface, and the LL dyad to produce a bulky topology with solubility in aprotic solvents. For several of the thus prepared bridged NDIs, two stable atropisomers[12,13,18,19] could be isolated as pairs of diastereomers (Figure 1a). Under reflux overnight in toluene, they did not isomerize.

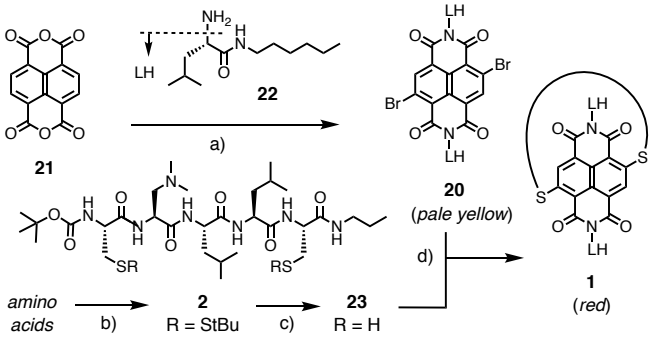

Scheme 1. Synthesis of catalyst **1**. (a) Standard NDI synthesis,[3,8] Scheme S1. (b) Standard peptide synthesis, Scheme S2. (c) PBu_3, TEA, TFE/H_2O 6:1, rt, 12 h. (d) TCEP, CH_3CN/buffer 3:1 (buffer: 60 mM NH_4HCO_3, pH 8.0), 65 ºC, 12 h, 14% (2 steps).

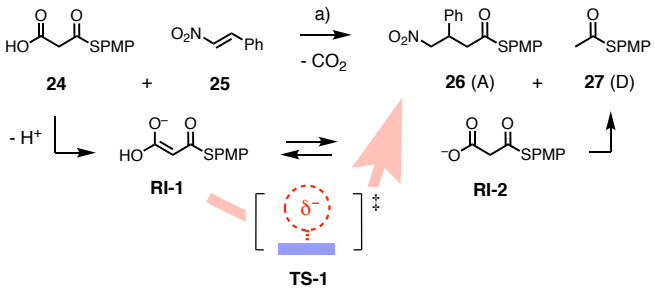

Figure 2. Benchmark reaction to probe for anion-π catalysis, with indication of enol and keto tautomers **RI-1** and **RI-2** of the first reactive intermediate, and schematic recognition of transition state **TS-1** by anion-π interactions, leading from enol **RI-1** to **26** (red arrow). a) 20 mol% catalyst **1**–**19**, 200 mM **24** and 2.0 M **25** in CD_2Cl_2 at 20 ºC. PMP = p-methoxyphenyl

The addition of malonic acid half thioesters **24** to enolate acceptors **25** has emerged as reliable benchmark reaction to assess anion-π catalysts (Figure 2).[3,6] The possible discrimination of planar, charge-delocalized enol tautomers and bent, charge-localized keto tautomers of the conjugate base of **24**, i.e., the first reactive intermediate of the reaction, on π-acidic aromatic surfaces attracted our attention early on.[7] By now such interactions have been shown in experiment and in theory to indeed change the chemoselectivity of the reaction in favor of the biologically and chemically relevant enolate

addition (A) product **26** compared to the simple but less relevant decarboxylation (D) product **27**.[3] The results are usually reported in A/D values, describing the yield of **26** divided by that of **27**.

Under standard experimental conditions in CD_2Cl_2, an A/D = 35 was obtained for C**B**LLC **1** (Table 1). Except for anion-π enzymes operating under different conditions,[1] this is the highest A/D value ever reported for anion-π catalysis.[3,10] For better comparison, we noticed that changes at high A/D are overappreciated compared to changes at low A/D. Moreover, they should be calibrated against a general standard such as TEA because intrinsic A/D_0 values also depend strongly on conditions.[3] We thus propose here to use qAD, the log of the measured A/D minus the log of the intrinsic A/D_0 with TEA. For C**B**LLC **1**, qAD = 0.94 was obtained (Table 1).

In the acyclic peptide control ^{p}C**B**LL^{p}C **2**, the activity of the NDI-stapled C**B**LLC **1** was completely lost (^{p}C stands for S*t*Bu protected C, Figure 1b, Table 1). Chemoselectivity was worse than with the TEA standard (qAD = –0.12). Increasing the space between π surface and peptide with one and two homocysteines in C**B**LL^{h}C **3** and ^{h}C**B**LL^{h}C **4** resulted in qAD = 0.40 and 0.51, respectively (Figure 3). Expansion of C**B**LLC **1** (qAD = 0.94) by one or two atoms thus clearly weakened anion-π catalysis. ^{h}C**B**LL^{h}C **4** was the first example in the series for which two atropisomers have been isolated in pure form (Figure 1a). While catalytic activity of these two diastereomers differed clearly (qAD = 0.51, 0.18), assignment of their structures was not possible without single crystals (Table 1).

Contraction of the peptide turn from C**B**LLC **1** to C**B**LC **5** nearly removed all activity (qAD = 0.18, Figure 3, Table 1). Exocyclic addition of the removed L at the N terminus of LC**B**LC **6** (qAD = 0.35) failed to restore the activity of the constitutional isomer C**B**LLC **1** (qAD = 0.94). Expansion of the peptide turn with one more L in the NDI-stapled C**B**LLLC hexapeptide **7** afforded similarly poor activity (qAD = 0.30). These losses in activity upon contraction and expansion implied that topologically correct stapling of an α-helix turn in C**B**LLC **1** is essential for powerful anion-π catalysis.

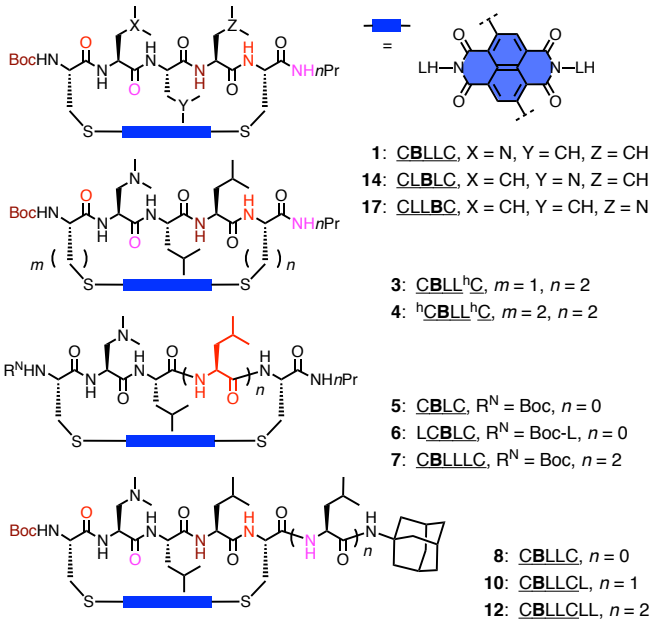

Figure 3. Full structure of selected catalysts. All catalyst structures are defined in Table 1.

The bulky, solubilizing adamantyl amide in CBLLC **8** did much not disturb anion-π catalysis (qAD = 0.72, Figure 3, Table 1). The massive drop in activity upon removal of the NDI was reproduced with ^{p}CBLL^{p}C **9** (qAD = 0.10). Exocyclic peptide elongation at the C terminus of the thus solubilized CBLLC **8** (qAD = 0.72) caused a strong increase in chemoselectivity. Hexapeptide CBLLCL **10** gave qAD = 0.97, heptapeptide CBLLCLL **12** gave qAD = 1.20. The acyclic, NDI-free controls of these longer ^{p}CBLL^{p}CL **11** and ^{p}CBLL^{p}CLL **13** remained consistently inactive (qAD = –0.12). The qAD = 1.20 obtained for the longest stapled peptide CBLLCLL **12** was the highest chemoselectivity observed in this study. Corresponding to A/D = 63, it indicates nearly complete suppression of the undesired decarboxylation product **27**. This record performance presumably originated from better organization of the stapled turn with additional hydrogen bonds to and from the exocyclic αhelix elongation. Additional contributions from remote control of anion-π catalysis by the strengthened α-helix macrodipole would be consistent with its orientation (Figures 1a, 3).[17]

Movement of the tertiary amine base **B** in C**B**LLC **1** (qAD = 0.94) by one position toward the C terminus in CL**B**LC **14** removed all activity (qAD = 0.00, Figure 3, Table 1). Indeed, the NDI-stapled **14** was less selective than the acyclic control ^{p}CL**B**L^{p}C **15** (qAD = 0.18). Hypersensitivity toward base position[3] supported that proximity to the π-acidic NDI surface is essential for C**B**LLC **1**, while in isomer CL**B**LC **14**, the base is too far from the NDI surface for operational anion-π catalysis. C-terminal modification to adamantyl amide failed to activate the CL**B**LC motif in **16** (qAD = 0.25).

Movement of the tertiary amine base **B** one more position toward the C terminus in CLL**B**C **17** (qAD = 0.68, 0.60) restored some but not all activity of the original C**B**LLC **1** (qAD = 0.94). Moreover, the acyclic control ^{p}CLL**B**^{p}C **18** (qAD = 0.30) was more selective than the acyclic original ^{p}C**B**LL^{p}C **2** (qAD = –0.14). These trends were consistent with the positioning of the amine bases according to ring current effects in ^{1}H NMR spectroscopy.[12] In the Cxx**B**C series, NDI stapling caused a downfield shift of the dimethyl amine resonances (CLL**B**C **17a/b**: 2.33/2.31 ppm, Figure S129/S132, ^{p}CLL**B**^{p}C **18**: 2.28 ppm, Figure S128). In contrast, those of C**B**xxC series shifted upfield upon NDI stapling (C**B**LLC **1**: 2.08 ppm, Figure S30, ^{p}C**B**LL^{p}C **2**: 2.25 ppm, Figure S18). These opposing ring current effects demonstrated that the positioning of the amine base right above the π surface, needed to stabilize the enolate intermediate by anion-π interactions as soon as it is produced,[3] is achieved only in C**B**LLC **1** (**TS-1**, Figure 2).

Asymmetric anion-π catalysis has been realized for many reactions.[3] However, anion-π catalysis of the addition of **24** to enolate acceptors **25** never occurred with significant enantioselectivities, except for anion-π enzymes.[3] Record values reported so far come from axially chiral NDI catalysts.[19] With peptide-bridged NDIs, enantioselectivities were better yet still not very impressive. The highest enantiomeric ratio *er* 66:34 was observed with CL**B**LC **14**, an NDI-stapled peptide that does not operate with anion-π catalysis and thus fails to influence chemoselectivity (qAD = 0.00). For the best performing C**B**LLC motif, *er* > 60:40 could be observed, while the intermediate CLL**B**C isomers gave the other enantiomer preferentially at *er* < 36:64. Comparison of *er* 65:35 of C**B**LLC **1**

with *er* 41:59 of acyclic ^{p}C**B**LL^{p}C **2** revealed that NDI stapling occurs with an inversion of the absolute enantioselectivity in this series, a trend that was confirmed by C**B**LLC **8** (*er* 61:39) against ^{p}C**B**LL^{p}C **9** (*er* 43:57). This inversion of configuration upon NDI stapling could be one of the reasons why the enantioselectivity of C**B**LLC anion-π catalysts is not as impressive as their chemoselectivity.

Reaction kinetics were measured first for the cyclic (C) C**B**LLC catalyst **1** compared to the acyclic, open (O) ^{p}C**B**LL^{p}C control **2**. Upon NDI stapling, the initial rate of the addition (A) product **26** increased by a factor $k_C^A/k_O^A = 3.3$ (Figure 4). For the decarboxylation (D) product **27**, NDI stapling decelerated the reaction by $k_C^D/k_O^D = 0.2$ (Figure 4). From these opposing trends, the contribution of anion-π catalysis to selective transition-state stabilization estimated to –6.9 kJ mol^{-1} (Table 2).

For the worst CL**B**LC isomer **14** compared to its acyclic control ^{p}CL**B**L^{p}C control **15**, rate enhancements for decarboxylation ($k_C^D/k_O^D = 3.6$) exceeded those for addition ($k_C^A/k_O^A = 1.9$, Table 2). With the amine base too far from the π surface, i.e., without anion-π catalysis, NDI stapling thus destabilized rather than stabilized the transition state of the reaction of interest by +1.5 kJ mol^{-1}. This result was is in agreement with qAD = 0.00 for CL**B**LC **14** being below qAD = 0.18 for ^{p}CL**B**L^{p}C **15** (Table 1).

Table 2. Kinetic analysis of selected catalysts.[a]

Entry	Cat[b]	Sequence[b]	k_C^A/k_O^A[c]	k_C^D/k_O^D[d]	$\Delta\Delta E_a$ [kJ mol^{-1}][e]
1	**1/2**	C**B**LLC	3.3	0.2	–6.9
2	**14/15**	CL**B**LC	1.9	3.6	+1.5
3	**17/18**	CLL**B**C	2.3	1.3	–1.5

[a] Conditions as in Figure 2. [b] Catalysts, sequences as in Table 1. [c] Rate enhancement for formation of addition (A) product **26**: Initial rate constant of the cyclic (C) catalyst divided by that for the acyclic (O) control, from NMR kinetics (Figure 4). [d] Same for decarboxylation (D) product

27. [e] Difference in activation energy ΔE_a of cyclic peptide compared to open control for addition product formation minus ΔE_a for decarboxylation product formation.

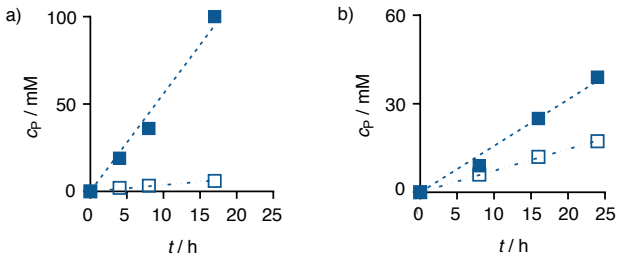

Figure 4. Initial velocities of the formation of products **26** (A, ■) and **27** (D, □) in the presence of a) **1** and b) **2** (Table 2).

For macrocycle CLL**B**C **17** measured against the acyclic ^{p}CLL**B**^{p}C **18**, rate enhancements for addition (k_C^A/k_O^A = 2.3) exceeded those for decarboxylation (k_C^D/k_O^D = 1.3, Table 2). The resulting –1.5 kJ mol^{-1} for transition-state recognition by CLL**B**C **17** was less impressive than the –6.9 kJ mol^{-1} of C**B**LLC **1** but of naturally better than the +1.5 kJ mol^{-1} of CL**B**LC **14**. This moderate kinetics performance of CLL**B**C **17** was consistent with an average chemoselectivity qAD ~ 0.64 compared to qAD = 0.94 for C**B**LLC **1** and qAD = 0.00 for CL**B**LC **14**.

To conclude, anion-π catalysis next to peptides consistently follows rational design and affords record activities. NDI stapling of α-helix-like turns is introduced as a chromogenic method of general appeal. It served as a convenient starting point to explore anion-π catalysis next to peptides. All deviations from the lead structure, from base misplacements to ring expansion, contraction and opening, are disastrous for catalysis. Exocyclic elongation of the turns into short, NDI-stapled α helices yields higher activities. The significant impact of these remote activity enhancers might originate from increased peptide organization and, perhaps, attractive contributions from □-helix macrodipoles to anion-π catalysis. These results encourage integration of the NDI-stapling motif into larger protein structures for different purposes, including anion-π enzymes.

Acknowledgements

We thank the NMR, the MS and the bioimaging platforms for services, and the University of Geneva, the Swiss National Centre of Competence in Research (NCCR) Chemical Biology, the NCCR Molecular Systems Engineering and the Swiss NSF for financial support.

Keywords: Anion-π catalysis • peptides • stapled peptides • naphthalenediimides • bridged aromatics

[1] Y. Cotelle, V. Lebrun, N. Sakai, T. R. Ward, S. Matile, *ACS Cent. Sci.* **2016**, *2*, 388–393.

[2] R. Wolfenden, M. J. Snider, *Acc. Chem. Res.* **2001**, *34*, 938–945.

[3] Y. Zhao, Y. Cotelle, L. Liu, J. López-Andarias, A.-B. Bornhof, M. Akamatsu, N. Sakai, S. Matile, *Acc. Chem. Res.* **2018**, *51*, 2255–2263.

[4] K. U. Wendt, G. E. Schulz, E. J. Corey, D. R. Liu, *Angew. Chem. Int. Ed.* **2000**, *39*, 2812–2833.

[5] a) C. R. Kennedy, S. Lin, E. N. Jacobsen, *Angew. Chem. Int. Ed.* **2016**, *55*, 12596–12624; b) E. Pahima, Q. Zhang, K. Tiefenbacher, D. T. Major, *J. Am. Chem. Soc.* **2019**, *141*, 6234–6246; c) C. M. Hong, R. G. Bergman, K. N. Raymond, F. D. Toste, *Acc. Chem. Res.* **2018**, *51*, 2447–2455.

[6] a) D.-X. Wang, M.-X. Wang, *Chimia* **2011**, *65*, 939−943; b) L. Li, Y.-J. Hong, Y. Lin, W.-C. Xiao, M.-J. Lin, *Chem. Commun.* **2018**, *54*, 11941–11944; c) Y. Kumar, S. Kumar, K. Mandal, P. Mukhopadhyay, *Angew. Chem. Int. Ed.* **2018**, *57*, 16318–16322; **d)** D.-H. Tuo, Y.-F. Ao, Q.-Q. Wang, D.-X. Wang, *Org. Lett.* **2019**, *21*, 7158–7162; e) W.-L. Huang, X.-D. Wang, S. Li, R. Zhang, Y.-F. Ao, J. Tang, Q.-Q. Wang, D.-X. Wang, *J. Org. Chem.* **2019**, *84*, 8859–8869; f) D.-H. Tuo, W. Liu, X.-Y. Wang, X.-D. Wang, Y.-F. Ao, Q.-Q. Wang, Z.-

Y. Li, D.-X. Wang, *J. Am. Chem. Soc.* **2019**, *141*, 1118–1125. g) J.-Z. Liao, L. Meng, J.-H. Jia, D. Liang, X.-L. Chen, R.-M. Yu, X.-F. Kuang, C.-Z. Lu, *Chem. Eur. J.* **2018**, *24*, 10498–10502; h) L. Li, Y.-J. Hong, D.-Y. Chen, W.-C. Xiao, M.-J. Lin, *Chem. Commun.* **2019**, *55*, 2364–2367; i) A. Bauzá, T. J. Mooibroek, A. Frontera, *ChemPhysChem* **2015**, *16*, 2496–2517; j) M. Giese, M. Albrecht, K. Rissanen, *Chem. Commun.* **2016**, *52*, 1778–1795; k) G. Bélanger-Chabot, A. Ali, F. P. Gabbaï, *Angew. Chem. Int. Ed.* **2017**, *56*, 9958–9961; l) P. Gamez, T. J. Mooibroek, S. J. Teat and J. Reedijk, *Acc. Chem. Res.* **2007**, *40*, 435–444; m) H. T. Chifotides, K. R. Dunbar, *Acc. Chem. Res.* **2013**, *46*, 894–906; n) Z. Yu, A. Erbas, F. Tantakitti, L. C. Palmer, J. A. Jackman, M. Olvera de la Cruz, N.-J. Cho, S. I. Stupp, *J. Am. Chem. Soc.* **2017**, *139*, 7823–7830; o) S. T. Schneebeli, M. Frasconi, Z. Liu, Y. Wu, D. M. Gardner, N. L. Strutt, C. Cheng, R. Carmieli, M. R. Wasielewski, J. F. Stoddart, *Angew. Chem. Int. Ed.* **2013**, *52*, 13100–13104; p) O. B. Berryman, D. W. Johnson, *Chem. Commun.* **2009**, *45*, 3143–3153; q) M. M. Watt, M. S. Collins, D. W. Johnson, *Acc. Chem. Res.* **2013**, *46*, 955–966.

[7] a) Y. Zhao, Y. Domoto, E. Orentas, C. Beuchat, D. Emery, J. Mareda, N. Sakai, S. Matile, *Angew. Chem. Int. Ed.* **2013**, *52*, 9940–9943; b) Y. Zhao, S. Benz, N. Sakai, S. Matile, *Chem. Sci.* **2015**, *6*, 6219–6223.

[8] X. Zhang, X. Hao, L. Liu, A.-T. Pham, J. López-Andarias, A. Frontera, N. Sakai, S. Matile, *J. Am. Chem. Soc.* **2018**, *140*, 17867–17871.

[9] a) M. Al Kobaisi, S. V. Bhosale, K. Latham, A. M. Raynor, S. V. Bhosale, *Chem. Rev.* **2016**, *116*, 11685–11796; b) S. V. Bhosale, C. H. Jani, S. J. Langford, *Chem. Soc. Rev.* **2008**, **37**, 331–342; **c)** J. Shukla, P. Mukhopadhyay, *Eur. J. Org. Chem.* **2019**, *2019*, 7770–7786; d) B. A. Ikkanda, S. A. Samuel, B. L. Iverson, *J. Org. Chem.* **2014**, *79*, 2029–2037; e) F. Würthner, S. Ahmed, C. Thalacker, T. Debaerdemaeker, *Chem. Eur. J.* **2002**, *8*, 4742–4750; f) G. D. Pantoş, J.-L. Wietor, J. K. M. Sanders, *Angew. Chem. Int. Ed.* **2007**, *46*, 2238–2240; g) S.

Hagihara, H. Tanaka, S. Matile, *J. Am. Chem. Soc.* **2008**, *130*, 5656–5657; h) N. Sakai, A. L. Sisson, T. Bürgi, S. Matile, *J. Am. Chem. Soc.* **2007**, *129*, 15758–15759; i) S. K. Keshri, A. Takai, T. Ishizuka, T. Kojima, M. Takeuchi, *Angew. Chem. Int.* **2020**, *59*, 5254–5258; j) S. Kuila, K. V. Rao, S. Garain, P. K. Samanta, S. Das, S. K. Pati, M. Eswaramoorthy, S. J. George, *Angew. Chem. Int. Ed.* **2018**, *57*, 17115–17119; k) K. Gayen, K. Basu, N. Nandi, K. S. Das, D. Hermida-Merino, I. W. Hamley, A. Banerjee, *ChemPlusChem* **2019**, *84*, 1673–1680.

[10] A.-B. Bornhof, M. Vázquez-Nakagawa, L. Rodríguez-Pérez, M. A. Herranz, N. Sakai, N. Martin, S. Matile, J. Lopez-Andarias, *Angew. Chem. Int. Ed.* **2019**, *58*, 16097–16100.

[11] a) L. Buglioni, M. M. Mastandrea, A. Frontera, M. A. Pericàs, *Chem. Eur. J.* **2019**, *25*, 11785–11790; b) X. Zhang, L. Liu, J. López-Andarias, C. Wang, N. Sakai, S. Matile, *Helv. Chim. Acta* **2018**, *101*, e1700288; c) K. S. Lee, J. R. Parquette, *Chem. Commun.* **2015**, *51*, 15653–15656. b) J. V. Alegre-Requena, E. Marqués-López, R. P. Herrera, *ACS Catal.* **2017**, *7*, 6430–6439; d) A. Berkessel, S. Das, D. Pekel, J. M. Neudörfl, *Angew. Chem. Int. Ed.* **2014**, *53*, 11660–11664; e) B. Reiß, H.-A. Wagenknecht, *Beilstein J. Org. Chem.* **2019**, *15*, 2043–2051.

[12] F. N. Miros, Y. Zhao, G. Sargsyan, M. Pupier, C. Besnard, C. Beuchat, J. Mareda, N. Sakai, S. Matile, *Chem. Eur. J.* **2016**, *22*, 2648–2657.

[13] a) W.-D. Woggon, *Acc. Chem. Res.* **2005**, *38*, 127–136; b) A. R. Battersby, A. D. Hamilton, *J. Chem. Soc. Chem. Commun.* **1980**, 117–119; c) M. M. Safont-Sempere, P. Osswald, M. Stolte, M. Grüne, M. Renz, M. Kaupp, K. Radacki, H. Braunschweig, F. Würthner, *J. Am. Chem. Soc.* **2011**, *133*, 9580–9591.

[14] a) A. L. Edwards, F. Wachter, M. Lammert, A. J. Huhn, J. Luccarelli, G. H. Bird, L. D. Walensky, *ACS Chem. Biol.* **2015**, *10*, 2149–2157; b) Q. Chu, R. E. Moellering, G. J. Hilinski, Y.-W. Kim, T. N. Grossmann, J. T.-H. Yeh, G. L. Verdine, *MedChemComm* **2015**,

6, 111–119; c) P. M. Cromm, J. Spiegel, T. N. Grossmann, *ACS Chem. Biol.* **2015**, *10*, 1362–1375; d) Y. H. Lau, P. de Andrade, Y. Wu, D. R. Spring, *Chem. Soc. Rev.* **2014**, *44*, 91–102; e) L. Nevola, E. Giralt, *Chem. Commun.* **2015**, *51*, 3302–3315.

[15] a) A. D. de Araujo, H. N. Hoang, W. M. Kok, F. Diness, P. Gupta, T. A. Hill, R. W. Driver, D. A. Price, S. Liras, D. P. Fairlie, *Angew. Chem. Int. Ed.* **2014**, *53*, 6965–6969; b) A. A. Beharry, G. A. Woolley, *Chem. Soc. Rev.* **2011**, *40*, 4422–4437; c) G. A. Woolley, *Acc. Chem. Res.* **2005**, *38*, 486–493; d) M. Dong, A. Babalhavaeji, S. Samanta, A. A. Beharry, G. A. Woolley, *Acc. Chem. Res.* **2015**, *48*, 2662–2670; e) D. A. Guarracino, J. A. Riordan, G. M. Barreto, A. L. Oldfield, C. M. Kouba, D. Agrinsoni, *Chem. Rev.* **2019**, *119*, 9915–9949; e) H. Jo, N. Meinhardt, Y. Wu, S. Kulkarni, X. Hu, K. E. Low, P. L. Davies, W. F. DeGrado, D. C. Greenbaum, *J. Am. Chem. Soc.* **2012**, *134*, 17704–17713; f) A. J. Rojas, C. Zhang, E. V. Vinogradova, N. H. Buchwald, J. Reilly, B. L. Pentelute, S. L. Buchwald, *Chem. Sci.* **2017**, *8*, 4257–4263; g) C. M. Grison, G. M. Burslem, J. A. Miles, L. K. A. Pilsl, D. J. Yeo, Z. Imani, S. L. Warriner, M. E. Webb, A. J. Wilson, *Chem. Sci.* **2017**, *8*, 5166–5171.

[16] a) S. S. Kale, C. Villequey, X.-D. Kong, A. Zorzi, K. Deyle, C. Heinis, *Nat. Chem.* **2018**, *10*, 715–723; b) C. Heinis, T. Rutherford, S. Freund, G. Winter, *Nat. Chem. Biol.* **2009**, *5*, 502–507; c) S. D. Appavoo, S. Huh, D. B. Diaz, A. K. Yudin, *Chem. Rev.* **2019**, *119*, 9724–9752.

[17] a) V. Diemer, L. Fischer, B. Kauffmann, G. Guichard, *Chem. Eur. J.* **2016**, *22*, 15684–15692; b) R. B. Hill, D. P. Raleigh, A. Lombardi, W. F. DeGrado, *Acc. Chem. Res.* **2000**, *33*, 745–754; c) W. S. Horne, S. H. Gellman, *Acc. Chem. Res.* **2008**, *41*, 1399–1408; d) B. A. F. Le Bailly, L. Byrne, J. Clayden, *Angew. Chem. Int. Ed.* **2016**, *55*, 2132–2136; e) J. A. Robinson, *Acc. Chem. Res.* **2008**, *41*, 1278–1288; f) L. Rocard, D. Wragg, S. A. Jobbins, L. Luciani, J. Wouters, S. Leoni, D. Bonifazi, *Chem. Eur. J.*, **2018**, *24*, 16136–16148.

[18] a) G. Bringmann, T. Gulder, T. A. M. Gulder, M. Breuning, *Chem. Rev.* **2011**, *111*, 563–639; b) A. Zask, J. Murphy and G. A. Ellestad, *Chirality* **2013**, *25*, 265–274; c) Y. S. Chong, B.

E. Dial, W. G. Burns, K. D. Shimizu, *Chem. Commun.* **2012**, *48*, 1296–1298; d) V. S. Raut, M. Jean, N. Vanthuyne, C. Roussel, T. Constantieux, C. Bressy, X. Bugaut, D. Bonne, J. Rodriguez, *J. Am. Chem. Soc.* **2017**, *139*, 2140–2143; e) E. Kumarasamy, R. Raghunathan, M. P. Sibi, J. Sivaguru, *Chem. Rev.* **2015**, *115*, 11239–11300; f) J. Wencel-Delord, A. Panossian, F. R. Leroux, F. Colobert, *Chem. Soc. Rev.* **2015**, *44*, 3418–3430.

[19] C. Wang, S. Matile, *Chem. Eur. J.* **2017**, *23*, 11955–11960.